

See discussions, stats, and author profiles for this publication at: <https://www.researchgate.net/publication/231637901>

# Photophysical Properties of the Pyrromethene 597 Dye: Solvent Effect

ARTICLE in THE JOURNAL OF PHYSICAL CHEMISTRY A · JUNE 2004

Impact Factor: 2.69 · DOI: 10.1021/jp0373898

CITATIONS

45

READS

90

5 AUTHORS, INCLUDING:



Jorge Bañuelos-Prieto

Universidad del País Vasco / Euskal Herriko U...

79 PUBLICATIONS 1,516 CITATIONS

SEE PROFILE



Fernando López Arbeloa

Universidad del País Vasco / Euskal Herriko U...

110 PUBLICATIONS 2,907 CITATIONS

SEE PROFILE



Virginia Martínez Martínez

Universidad del País Vasco / Euskal Herriko U...

45 PUBLICATIONS 1,174 CITATIONS

SEE PROFILE

## ARTICLES

### Photophysical Properties of the Pyrromethene 597 Dye: Solvent Effect

J. Bañuelos Prieto, F. López Arbeloa,\* Virginia Martínez Martínez, T. Arbeloa López, and I. López Arbeloa

*Departamento Química Física, Universidad País Vasco-EHU, Apartado 644, 48080-Bilbao, Spain*

*Received: November 7, 2003*

UV–vis absorption spectroscopy and fluorescence (steady-state and time-resolved) techniques were used to study the photophysical properties of the pyrromethene 597 (PM597) dye in several solvents, which include a wide range of apolar, polar, and protic media. This dye presents a lower fluorescence quantum yield than the well-known PM567 dye because of an increase in the nonradiative deactivation rate constant. This is attributed to a loss of planarity in the excited state provided by the steric hindrance of the *tert*-butyl groups at positions 2 and 6 of the chromophore core. Such a geometrical change in the excited state leads to an important Stokes shift, reducing the reabsorption and reemission effects in the detected emission in highly concentrated dye solutions. The highest fluorescence quantum yield of PM597 is observed in polar media.

#### Introduction

Pyrromethenes are a laser dye family synthesized at the end of the 1980s as a result of continuous efforts to achieve dye lasers with improved laser performance.<sup>1–3</sup> Pyrromethenes are based on the fluoroboration of two pyrrole groups linked by a conjugated chain, giving rise to the dipyrromethene-BF<sub>2</sub> (PM) complexes, which can be classified as cyclic cyanines. These dyes show very interesting and encouraging photophysical properties.<sup>4–10</sup> They emit in the green-yellow and red part of the visible electromagnetic spectrum with a high molar absorption coefficient (around 10<sup>5</sup> M<sup>-1</sup> cm<sup>-1</sup>) and a fluorescence quantum yield, in some cases, near unity.<sup>11</sup> They also present even better laser action than rhodamine dyes,<sup>12,13</sup> which are considered the benchmark in laser performance.

Several factors contribute to the best laser performance of pyrromethene with respect to rhodamine as laser dyes: (1) low triplet–triplet absorption capacity at the lasing spectral region,<sup>14</sup> which reduces the losses in the resonator cavity; (2) a poor tendency to self-aggregate in organic solvents,<sup>9,15,16</sup> avoiding

the fluorescence quenching of the monomer emission by the presence of H aggregates in highly concentrated solutions, as was observed in rhodamine dyes;<sup>17</sup> and (3) their high photostability,<sup>18–20</sup> which improves the lifetime of the laser action with respect to that of rhodamines.<sup>21</sup> Owing to these properties, PM dyes have been successfully incorporated into different solid matrixes (polymers, silica, etc.),<sup>22–27</sup> to develop solid-state syntonizable dye lasers.

In previous papers, good correlations between photophysical properties and laser characteristics were observed for PM dyes in liquid solutions and in polymeric matrixes,<sup>15,16,27,28</sup> indicating that the laser behavior is a consequence of the photophysical properties. Indeed, the evolution of the fluorescence wavelength and quantum yield with several environmental factors was similar to that observed for the laser band and efficiency, respectively. The Stokes shift modifies the lasing performance<sup>29</sup> in highly concentrated dye solutions because it affects the reabsorption and reemission phenomena, which shifts the emission band to longer wavelengths and reduces its efficiency.<sup>30</sup> Consequently, the study of the photophysical properties of PM dyes can be a successful tool for the prediction of the best

\* Corresponding author. Phone: +34 94 601 59 71. Fax: +34 94 601 35 00. E-mail: qfploarf@lg.ehu.es.

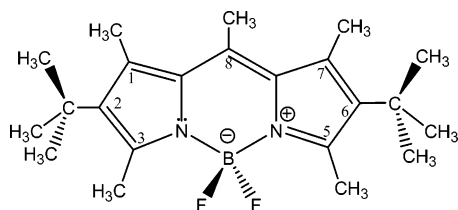


Figure 1. Molecular structure of PM597.

environmental conditions to optimize the laser action of syntonizable dye lasers.

In the present paper, the photophysical properties of pyrromethene 597, PM597, (Figure 1) are investigated in a wide variety of solvents, including apolar, polar, and protic solvents. This dye, with five methyl groups at positions 1, 3, 5, 7, and 8 of the PM chromophore, has a similar molecular structure to that of the more extensively used pyrromethene 567 (PM567) dye but with *tert*-butyl groups at positions 2 and 6 instead of ethyl groups. The solvent effects on the absorption and fluorescence bands are analyzed by a multicomponent linear regression in which several solvent parameters are simultaneously analyzed. The fluorescence quantum yield and the Stokes shift are analyzed to look for the best conditions to improve the lasing efficiencies of this dye.

## Experimental Section

Pyrromethene 597 (laser grade) was supplied by Exciton and used as received. All solvents (Merck, Aldrich, or Sigma) were spectroscopic grade and were used without further purification. Dilute solutions of PM597 in several solvents were prepared by taking the appropriate volume of a concentrated stock PM597 solution in acetone and adding the corresponding solvent after solvent vacuum evaporation.

UV–vis absorption and fluorescence (after excitation at 495 nm) spectra were recorded on a CARY 4E spectrophotometer and a Shimadzu RF-5000 spectrofluorimeter, respectively. Fluorescence spectra were corrected from the monochromator wavelength dependence and the photomultiplier sensibility. Fluorescence quantum yields ( $\phi$ ) were determined by means of the corrected fluorescence spectra of a dilute solution of PM567 in methanol as a reference ( $\phi = 0.91$  at 20 °C)<sup>15</sup> and by taking into account the solvent refractive index. Radiative decay curves were recorded by means of a time-correlated single-photon counting technique (Edinburgh Instruments model  $\eta$ F900). Emission was monitored at around 565 nm after excitation at 495 nm by means of a hydrogen flash lamp with 1.5-ns fwhm pulses and a 40-kHz repetition rate.

The photophysical properties of PM597 were recorded in dilute dye concentrations ( $2 \times 10^{-6}$  M) using a 1-cm optical pathway. The fluorescence decay curves were analyzed as monoexponentials ( $\chi^2 < 1.2$ ), and the fluorescence decay time ( $\tau$ ) was obtained from the slope. The estimated errors in the determination of  $\phi$  and  $\tau$  were 5 and 1%, respectively. The rate constant for the radiative ( $k_{\text{r}}$ ) and nonradiative ( $k_{\text{nr}}$ ) deactivation pathways were calculated to be:  $k_{\text{r}} = \phi/\tau$  and  $k_{\text{nr}} = (1 - \phi)/\tau$ . The temperature was always kept at  $20 \pm 0.2$  °C. For highly concentrated dye solutions ( $\leq 10^{-3}$  M), we used the front-face (reflection) configuration by orientating 0.1-, 0.01-, and 0.001-cm pathway cuvettes to 35 and 55° with respect to the excitation beam and the emission arm, respectively.

Quantum mechanical calculations were performed by the AM1 semiempirical method<sup>31</sup> as implemented in the MOPAC2000 software<sup>32</sup> that is included in the CHEM3D 7.0.0 package (CambridgeSoft). The geometry optimization was made

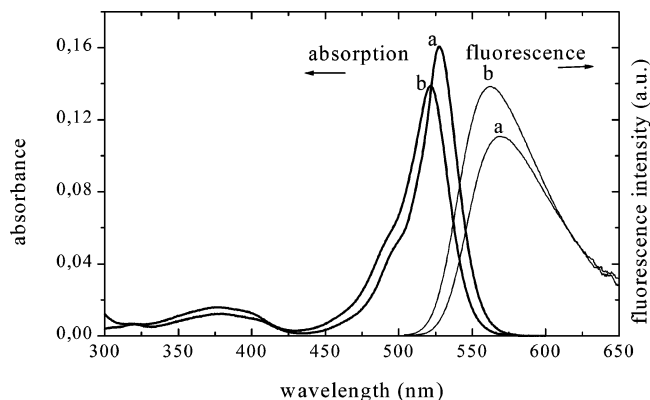


Figure 2. Absorption (bold lines) and normalized to the fluorescence quantum yield fluorescence (thin lines) spectra of PM597 ( $2 \times 10^{-6}$  M) in isooctane (a) and 2,2,2-trifluoroethanol (b).

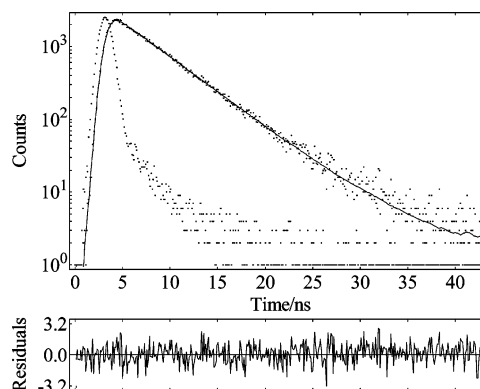


Figure 3. Fluorescence decay curve of PM597  $2 \times 10^{-6}$  M in acetone at 20 °C. The signal is deconvoluted as a monoexponential decay (statistical parameters:  $\chi^2 = 1.04$  and D. W. = 2.01). The residuals of the deconvoluted points are also included.

using the Eigenvector Following<sup>33</sup> routine, and the minimum gradient for convergence was imposed at 0.01 kcal/mol Å. The calculated geometry was considered to be adequately optimized when the analysis of the vibrational frequencies did not give any negative frequency.

## Results and Discussion

UV–vis absorption and fluorescence spectra of the PM597 dye are shown in Figure 2. In apolar solvents, the main absorption band is centered around 525 nm with a high molar absorption coefficient ( $\epsilon \approx 8 \times 10^4$  M<sup>-1</sup> cm<sup>-1</sup>), whereas the fluorescence spectrum is centered around 565 nm with a fluorescence quantum yield around 0.40. Figure 3 shows the fluorescence decay curve of the PM597 dye, which can be analyzed as a monoexponential decay ( $\chi^2 < 1.2$ ) with a fluorescence lifetime of  $\sim 4.2$  ns.

The absorption and fluorescence spectra of PM597 are shifted to lower energies with respect to those of the well-known PM567<sup>15</sup> in a common solvent. These spectral shifts are attributed to the higher inductive electron-donor character of the alkyl groups at positions 2 and 6, which is higher for *tert*-butyl groups (PM597) than for ethyl groups (PM567). However, the bathochromic shift is lower in the absorption (7 nm) than in the fluorescence (30 nm) bands, providing a larger Stokes shift for the PM597 dye ( $\sim 1350$  cm<sup>-1</sup>) than for the PM567 dye ( $\sim 600$  cm<sup>-1</sup>). These results suggest an important geometrical rearrangement in the S<sub>1</sub> excited state for the former dye. Indeed, PM dyes present Stokes shifts that are usually  $< 700$  cm<sup>-1</sup>,<sup>4,6,9,15</sup> indicating a similar geometric structure for the dye

TABLE 1: Photophysics of the PM597 Dye in Dilute Solutions ( $2 \times 10^{-6}$  M) of Several Solvents<sup>a</sup>

	solvent	$\lambda_{ab}$ ( $\pm 0.1$ nm)	$\lambda_{fl}$ ( $\pm 0.4$ nm)	$\Delta\nu_{St}$ ( $\text{cm}^{-1}$ )	$\phi$ ( $\pm 0.05$ )	$\tau$ ( $\pm 0.01$ ns)	$\epsilon_{max}$ ( $10^4 \text{ M}^{-1} \text{ cm}^{-1}$ )	$k_{fl}$ ( $10^8 \text{ s}^{-1}$ )	$k_{nr}$ ( $10^8 \text{ s}^{-1}$ )
1	2-methylbutane	527.1	569.0	1395	0.40	4.19	8.20	0.95	1.43
2	hexane	527.5	567.8	1345	0.43	4.35	8.25	0.98	1.31
3	c-hexane	529.0	571.2	1395	0.32	3.91	8.10	0.81	1.74
4	isooctane	527.5	569.0	1380	0.40	4.43	8.05	0.90	1.35
5	diethyl ether	525.1	565.4	1355	0.43	4.27	7.90	1.00	1.33
6	1,4-dioxane	525.1	565.4	1355	0.40	4.37	7.85	0.91	1.37
7	THF <sup>b</sup>	525.1	566.6	1395	0.37	4.15	7.75	0.89	1.51
8	DMF <sup>b</sup>	524.0	565.4	1395	0.35	4.69	5.89	0.74	1.38
9	acetone	522.5	563.6	1395	0.44	4.34	7.44	1.01	1.29
10	2-pentanone	523.7	562.6	1320	0.46	4.54	6.13	1.01	1.24
11	methyl formate	522.3	560.6	1310	0.47	4.45	7.55	1.05	1.19
12	methyl acetate	522.5	561.8	1340	0.48	4.44	7.85	1.08	1.17
13	ethyl acetate	523.2	562.4	1330	0.44	4.31	7.67	1.02	1.23
14	butyl acetate	524.3	564.6	1360	0.43	4.51	7.85	0.95	1.26
15	acetonitrile	520.8	560.6	1365	0.44	4.27	7.60	1.03	1.31
16	1-octanol	527.3	565.0	1265	0.41	4.68	7.70	0.87	1.26
17	1-hexanol	526.7	565.4	1300	0.42	4.59	7.55	0.71	1.26
18	1-butanol	526.1	566.6	1360	0.39	4.33	7.70	0.90	1.40
19	1-propanol	525.3	564.6	1325	0.39	4.19	7.75	0.93	1.45
20	ethanol	524.3	563.2	1315	0.43	4.09	7.63	1.05	1.39
21	methanol	522.9	561.2	1305	0.48	4.21	7.58	1.14	1.23
22	F <sub>3</sub> -ethanol <sup>b</sup>	521.6	561.2	1355	0.49	4.64	7.01	1.05	1.10

<sup>a</sup> Wavelength of absorption and fluorescence maximum ( $\lambda_{ab}$  and  $\lambda_{fl}$ ), Stokes shift ( $\Delta\nu_{St}$ ), molar absorption coefficient ( $\epsilon_{max}$ ), fluorescence quantum yield ( $\phi$ ), and lifetime ( $\tau$ ), rate constants of radiative ( $k_{fl}$ ) and non-radiative ( $k_{nr}$ ) deactivation. <sup>b</sup> THF— tetrahydrofuran; DMF— dimethylformamide; F<sub>3</sub>-ethanol— 2,2,2-trifluoroethanol.

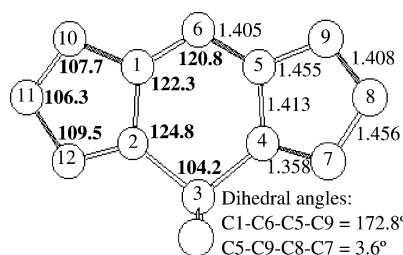


**Figure 4.** Optimized structure of PM597 by the semiempirical AM1 method. The bond lengths (in Å) and the bond angles (bold numbers) are included within the molecular structure, and some representative dihedral angles indicate the planarity of the chromophore.

in the excited state and the ground state. The long Stokes shift of PM597 seems to be a characteristic of this dye; more concretely, it should be related to the bulkiness of the *tert*-butyl groups at positions 2 and 6.

Figure 4 shows the optimized geometrical structure of PM597 in the ground state that was calculated by the semiempirical AM1 method. The PM chromophoric system presents some deviation from planarity, as reflected in the dihedral angle between the two pyrrole units (dihedral angle C1–C6–C5–C9 = 172.8°) and the distortion angle of the pyrrole rings (dihedral angle C7–C8–C9–C5 = 3.6°). Both pyrrole units are nearly planar for the PM567 dye (dihedral angle C7–C8–C9–C5 = 0.3°), indicating that the loss of planarity for the PM597 is due to steric hindrance between the 2- (and 6-) *tert*-butyl groups with the corresponding adjacent 1- and 3- (and 5- and 7-) methyl groups. Indeed, X-ray data support this assumption because this dihedral angle is 3.8° for PM597 and 0.8° for PM567.<sup>34</sup> The distortion from planarity of the pyrrole rings in PM597 is higher in the excited state because the corresponding dihedral angle C7–C8–C9–C5 is calculated to be ~4.8° by the CIS method.<sup>35</sup>

The higher bathochromic shift observed in the fluorescence band of PM597, with respect to the parent PM567, can be interpreted by the so-called Brunings–Corwin effect.<sup>36</sup> Because the distortion of the geometry in the excited state implies a decrease in the resonance energy, the fluorescence band is

bathochromically shifted to a higher extent than the absorption band. Moreover, the loss of planarity in the excited state of the PM597 dye could explain the lower fluorescence quantum yield (0.40) and lifetime (4.2 ns) in apolar solvents, with respect to those of the PM567 dye (~0.80 and 5.9 ns<sup>15</sup>), owing to an increase in the nonradiative processes in PM597, as discussed below.

However, the shape of the absorption band of PM597 is independent of the dye concentration ( $<10^{-3}$  M in 0.01-cm-pathway cuvettes), at least in c-hexane, ethyl acetate, acetone, ethanol, methanol, and trifluoroethanol, suggesting the poor aggregation tendency of the PM597 dye in this concentration range. This is common in PM dyes in liquid organic solutions, and it is a suitable behavior in the performance of active media of dye lasers. Indeed, high dye concentration is necessary to bring about laser action, and the presence of aggregates could drastically reduce the fluorescence quantum yield owing to the efficient quenching of the monomer fluorescence by the aggregates.<sup>17</sup> However, experimental data indicate that the fluorescence band is shifted to lower energies by increasing the PM597 concentration. This bathochromic shift is attributed to reabsorption and reemission phenomena<sup>30</sup> because the displacement is reduced by using narrower cuvettes and returns to the value in dilute solutions for 0.001-cm pathway cuvettes. This result corroborates the importance of registering photophysical properties in dilute solutions.

Table 1 lists the photophysical properties of PM597 in several solvents, including apolar, polar, and polar protic media. Both absorption and fluorescence bands are shifted toward higher energies by increasing the solvent polarity. The hypsochromic shift is commonly observed in other pyrromethene dyes<sup>9,15,16</sup> and suggests a diminution in the dipole moment of the chromophore upon excitation. Quantum mechanical calculations at the semiempirical AM1 level confirm this assumption. Indeed, the dipole moment of PM597 in the ground state is located in the short molecular axis (transversal axis). Figure 5 shows the calculated contour maps for the electronic distribution of the HOMO and LUMO states by the AM1 method. The electron density at position 8 is augmented in the LUMO with respect

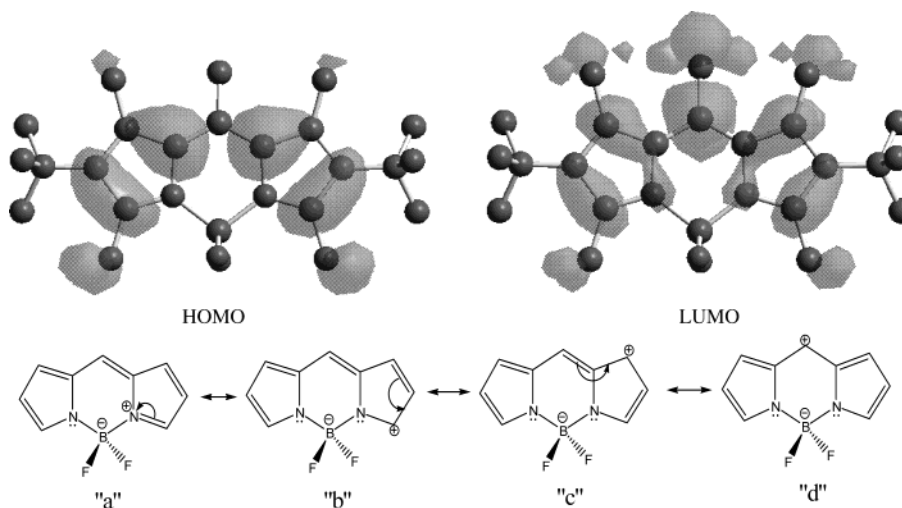


**Figure 5.** HOMO and LUMO contour maps calculated by the AM1 method and resonance structures of the PM597 chromophoric core. Other symmetrical resonance structures are not included.

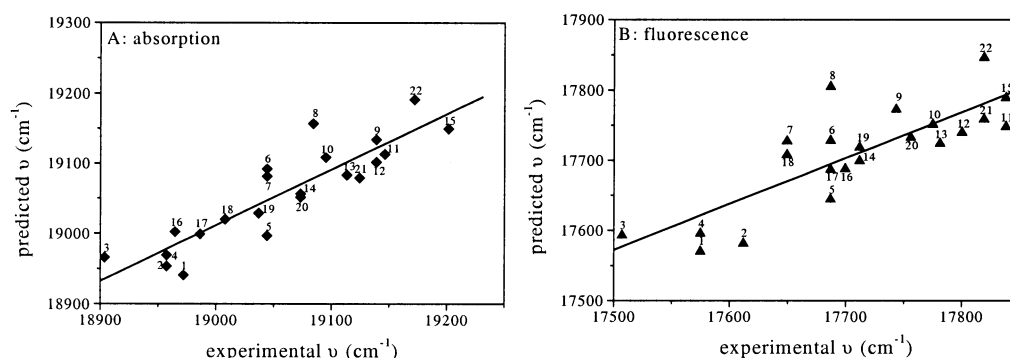


**Figure 6.** Correlation between the experimental absorption (A) and fluorescence (B) wavenumber with the predicted values obtained by a multicomponent linear regression using the  $\pi^*$ -,  $\alpha$ -, and  $\beta$ -scale (Taft) solvent parameters. Solvent numbers are those in Table 1.

to that in the HOMO state. Taking into account the resonance structures of the PM chromophore (Figure 5), we observed that the resonance structure "d" has the largest charge separation along the short molecule axis. Consequently, its contribution would be more important in the  $S_0$  ground state than in the  $S_1$  excited states. Thus, a polar solvent would stabilize the  $S_0$  state more extensively than the  $S_1$  state, thereby increasing the energy gap between both states and explaining the hypsochromic shifts. The relatively low hypsochromic shift observed in the absorption and fluorescence bands of PM597 ( $\sim 8$  nm from the lowest to the highest polar solvents) is assigned to the relatively low variation of the dipole moment in the  $S_0$  (3.53 D) and  $S_1$  (2.37 D) states. Indeed, the small dipole moments characterizing the  $S_0$  and  $S_1$  states of PM dyes are responsible for the weak solvent effects on the spectral properties of these dyes.<sup>37</sup>

To analyze the solvatochromic effects, we checked several methods<sup>38–40</sup>. Neither the absorption nor the fluorescence wavenumbers linearly correlate with the Lippert parameter  $\Delta f(\epsilon, n^2)$ ,<sup>41</sup> which considers the solvent polarity/polarizability, or with the Reichardt parameter  $E_T^N(30)$ ,<sup>39,42</sup> which takes into account several solvent properties (polarity and H-bond donor capacity) in a common parameter. For these reasons, a multi-parameter correlation analysis is employed in which a physicochemical property is linearly correlated with several solvent parameters by means of eq 1:

$$(XYZ) = (XYZ)_0 + c_a A + c_b B + c_c C + \dots \quad (1)$$

where  $(XYZ)_0$  is the physicochemical property in an inert solvent

and  $c_a$ ,  $c_b$ ,  $c_c$ , and so forth are the adjusted coefficients that reflect the dependence of the physicochemical property (XYZ) on several solvent properties. Solvent properties that mainly affect the photophysical properties of aromatic compounds are polarity, H-bond donor capacity, and electron donor ability. Different scales for such parameters can be found in the literature: Taft et al.<sup>43</sup> propose the  $\pi^*$ ,  $\alpha$ , and  $\beta$  scales, whereas more recently Catalan et al.<sup>44</sup> suggest the SPP<sup>N</sup>, SA, and SB scales to describe, respectively, the polarity/polarizability and the acidity and basicity of the solvent.

Figure 6 shows the obtained correlations between the absorption and fluorescence wavenumbers calculated by the multicomponent linear regression employing the Taft-proposed solvent parameters and the experimental values listed in Table 1. Table 2 lists the obtained adjustment and correlation coefficients by the Taft and Catalan parameters. The two sets of solvent parameters give qualitatively similar results. The values of the correlation coefficient are not close to unity because the experimental errors in the absorption ( $\pm 0.1$  nm) and fluorescence ( $\pm 0.4$  nm) wavelengths lead to a high dispersion of the experimental data through the linearity in a very low spectra interval ( $\sim 8$  nm) from the most apolar to the most polar solvents.

The dominant coefficient affecting the absorption and fluorescence bands of PM597 is that describing the polarity/polarizability of the solvent,  $c_{\pi^*}$  or  $c_{SPP^N}$ , and having a positive value (Table 2), corroborating the above-mentioned hypsochromic shifts with the solvent polarity. The coefficient controlling



**TABLE 2: Adjusted Coefficients ( $(v_x)_0$ ,  $c_a$ ,  $c_b$ , and  $c_c$ ) and Correlation Coefficients ( $r$ ) for the Multilinear Regression Analysis of the Absorption  $v_{ab}$  and Fluorescence  $v_f$  Wavenumbers and Stokes Shift ( $\Delta v_{St}$ ) of the PM597 Dye with the Solvent Polarity/Polarizability, and the Acid and Base Capacity Using the Taft ( $\pi^*$ ,  $\alpha$ , and  $\beta$ )<sup>43</sup> and the Catalan (SPP<sup>N</sup>, SA and SB)<sup>44</sup> Scales, Respectively**

$(v_x)$	$(v_x)_0$ (cm <sup>-1</sup> )	$c_{\pi^*}$	$c_\alpha$	$c_\beta$	$r$
$v_{ab}$	18 970 ( $\pm 20$ )	300 ( $\pm 40$ )		-110 ( $\pm 35$ )	0.89
$v_f$	17 590 ( $\pm 25$ )	280 ( $\pm 50$ )	30 ( $\pm 25$ )	-50 ( $\pm 50$ )	0.81
$\Delta v_{St} = v_{ab} - v_f$	1370 ( $\pm 15$ )		-30 ( $\pm 15$ )	-60 ( $\pm 30$ )	0.61

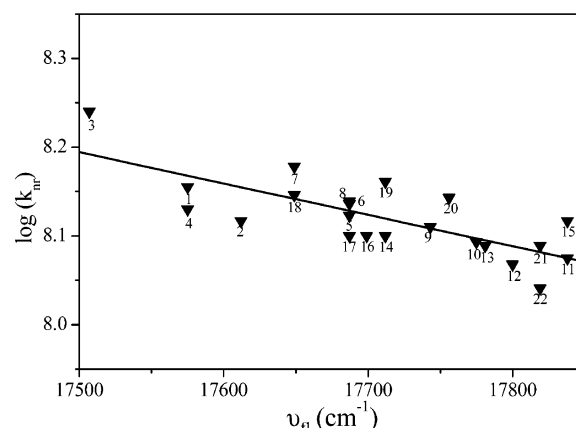
  

$(v_x)$	$(v_x)_0$ (cm <sup>-1</sup> )	$c_{SPP^N}$	$c_{SA}$	$c_{SB}$	$r$
$v_{ab}$	18 630 ( $\pm 60$ )	670 ( $\pm 100$ )	-40 ( $\pm 30$ )	-180 ( $\pm 45$ )	0.88
$v_f$	17 300 ( $\pm 90$ )	570 ( $\pm 150$ )	30 ( $\pm 30$ )	-85 ( $\pm 60$ )	0.78
$\Delta v_{St} = v_{ab} - v_f$	1325 ( $\pm 45$ )	100 ( $\pm 70$ )	-70 ( $\pm 30$ )	-95 ( $\pm 30$ )	0.71

the H-donor capacity or acidity of the solvent,  $c_\alpha$  or  $c_{SA}$ , is the lowest coefficient (Table 2); therefore, the solvent acidity does not play an important role in absorption and fluorescence displacements. The adjusted coefficient representing the electron-releasing ability or basicity of the solvent,  $c_\beta$  or  $c_{SB}$ , has a negative value (Table 2), suggesting that the absorption and fluorescence bands shift to lower energies with the increasing electron-donating ability of the solvent. This effect can be interpreted in terms of the stabilization of the resonance structures of the chromophore (Figure 5). Resonance structure "a" has the positive charge located at the nitrogen atom, and it will be stabilized in basic solvents because this resonance structure is predominant in the  $S_1$  state, as discussed above, and the stabilization of the  $S_1$  state with the solvent basicity would be more important than that of the  $S_0$  state. Consequently, the energy gap between the  $S_1$  and  $S_0$  states decreases, and the absorption and fluorescence wavelengths shift to longer wavelengths with increasing solvent basicity.

However, the fluorescence quantum yield and lifetime values of PM597 are, in general, lower than those observed in others pyrromethenes<sup>9,15,16</sup> in a common solvent. This is a consequence of an important augmentation in the rate constant of the nonradiative deactivation ( $k_{nr} \approx 1 \times 10^8$  s<sup>-1</sup>, Table 1, for PM597 versus  $k_{nr} \approx 0.3 \times 10^8$  s<sup>-1</sup> for PM567<sup>15</sup>) rather than a decrease in the radiative deactivation, which remains similar to that of other PM dyes ( $\sim 10^8$  s<sup>-1</sup>, Table 1). Consequently the  $S_0$ – $S_1$  electronic transition of PM597 is still high, as is also reflected in its high molar absorption coefficient (Table 1). The solvent also affects the fluorescence quantum yield and lifetime of PM597, and  $\phi$  and  $\tau$  values increase in polar/protic solvents (Table 1), although a general tendency in both parameters with respect to the solvent viscosity is not observed. These results indicate an extra nonradiative deactivation of PM597, which is not governed by the solvent viscosity. Figure 7 shows a correlation between the  $k_{nr}$  value and the fluorescence wavenumber of PM597 by changing the nature of the solvent, indicating similar solvent parameters affecting both photophysical characteristics, as was also proposed for other aromatic systems.<sup>45–49</sup>

It is well known that the flexibility/rigidity of the dye can control the mechanics of internal conversion. The flexibility/rigidity of the aromatic compounds can be analyzed in terms of the planarity of the  $\pi$ -electron system.<sup>50,51</sup> This loss of planarity, especially in the excited state, implies a less rigid structure, and the excitation energy is more easily converted to vibrational energy and dissipated as heat, enhancing the internal conversion processes. Indeed, Drexhage<sup>50</sup> pointed out that the structure loosens up in some dyes upon excitation, enhancing the nonradiative deactivation processes. More concretely, the torsion of the pyrrole rings of PM597 is assigned to the steric hindrance between the bulky *tert*-butyl group at positions 2 and

**Figure 7.** Correlation between the rate constant of nonradiative deactivation ( $\log k_{nr}$ ) with the fluorescence wavenumbers ( $v_f$ ) in several solvents. Solvent numbers are given in Table 1.

6 with the respective 1 and 3 and 5 and 7 adjacent methyl groups. Such a distortion from planarity leads to an augmentation of the nonradiative deactivation. Boyer et al.<sup>3</sup> also referred to the nonplanarity of the PM chromophore provided by bulky substituents to explain the low fluorescence quantum yield of some PM and related compounds.

The present photophysical characteristics of PM597 would suggest a lower lasing efficiency of this dye with respect to that of other dyes because of its lower fluorescence quantum yield. However, high optical densities are required to produce laser signals and, under these conditions, the losses at the resonator cavity by the reabsorption and reemission effects can be important. PM597 dye is characterized by a higher Stokes shift with respect to that of other PM dyes, for instance, twice that observed in PM567, which would reduce the losses at the resonator cavity by reabsorption and reemission effects, governed by the overlap between the absorption and emission spectra.<sup>30</sup> Therefore, the low fluorescence quantum yield of the PM597 dye could, to some extent, be compensated by its high Stokes shift, and high laser efficiencies for PM597, similar to those for PM567, are obtained.<sup>11,23,24,52–55</sup>

Because the Stokes shift of the PM597 dye is nearly solvent-independent, polar solvents, where the highest fluorescence quantum yield values are observed, are recommended to achieve the highest laser efficiencies of PM597 in liquid media.

## Conclusions

The presence of bulky *tert*-butyl groups in the PM chromophore core originates a distortion from planarity in the pyrrole units, mainly in the excited state, which leads to an increase in the rate constant of nonradiative deactivation and in the Stokes shift. Both photophysical factors have an opposite

effect on the lasing efficiency of the dye. Thus, the increase in the losses of the resonator cavity due to the augmentation in the nonradiative processes could be compensated to some extent by a reduction in the reabsorption and reemission losses, owing to the high Stokes shift. From this photophysical study, polar solvents are recommended to obtain the highest laser efficiencies of PM597 in liquid media.

**Acknowledgment.** This work is supported by the Spanish MCyT Minister (project no. MAT2000-1361-C04-02). J.B.P. and V.M.M. thank the University of the Basque Country UPV/EHU and the Spanish MECyD Minister, respectively, for research grants.

## References and Notes

- (1) Shah, M.; Thangaraj, K.; Soong, M.-L.; Welford, L. T.; Boyer, J. H.; Politzer, I. R.; Pavlopoulos, T. G. *Heteroat. Chem.* **1990**, *1*, 389.
- (2) Pavlopoulos, T. G.; Boyer, J. H.; Thangaraj, K.; Sathyamoorthi, G.; Soong, M.-L. *Appl. Opt.* **1992**, *31*, 7089.
- (3) Boyer, J. H.; Haag, A. M.; Sathyamoorthi, G.; Soong, M.-L.; Thangaraj, K.; Pavlopoulos, T. G. *Heteroat. Chem.* **1993**, *4*, 39.
- (4) Karolin, J.; Johansson, L. B. A.; Strandberg, L.; Ny, T. *J. Am. Chem. Soc.* **1994**, *116*, 7801.
- (5) Li, F.; Yang, S. I.; Ciringh, Y.; Seth, J.; Martin, C. H.; Singh, D. L.; Kim, D.; Birge, R. R.; Bocian, D. F.; Holten, D.; Lindsey, J. S. *J. Am. Chem. Soc.* **1998**, *120*, 10001.
- (6) Kollmannsberger, M.; Prurack, K.; Resch-Genger, U.; Daub, J. *J. Phys. Chem. A* **1998**, *102*, 10211.
- (7) Liang, F.; Zeng, H.; Sun, Z.; Yuan, Y.; Yao, Z.; Xu, Z. *J. Opt. Soc. Am. B* **2001**, *18*, 1841.
- (8) Wada, M.; Ito, S.; Uno, H.; Murashima, T.; Ono, N.; Urano, T.; Urano, Y. *Tetrahedron Lett.* **2001**, *42*, 6711.
- (9) Costela, A.; García-Moreno, I.; Gómez, C.; Sastre, R.; Amat-Guerri, F.; Liras, M.; López Arbeloa, F.; Bañuelos Prieto, J.; López Arbeloa, I. *J. Phys. Chem. A* **2002**, *106*, 7736.
- (10) Toebe, P.; Zhang, H.; Trieflinger, C.; Daub, J.; Glasbeek, M. *Chem. Phys. Lett.* **2003**, *368*, 66.
- (11) Partridge, W. P.; Laurendeau, N. M.; Johnson, C. C.; Steppel, R. N. *Opt. Lett.* **1994**, *19*, 1630.
- (12) Guggenheimer, S. C.; Boyer, J. H.; Thangaraj, K.; Shah, M.; Soong, M.-L.; Pavlopoulos, T. G. *Appl. Opt.* **1993**, *32*, 3942.
- (13) Hermes, R. E.; Allik, T. H.; Chnadra, S.; Hutchinson, J. A. *Appl. Phys. Lett.* **1993**, *63*, 877.
- (14) Boyer, J. H.; Haag, A. M.; Soong, M.-L.; Thangaraj, K.; Pavlopoulos, T. G. *Appl. Opt.* **1991**, *30*, 3788.
- (15) López Arbeloa, F.; López Arbeloa, T.; López Arbeloa, I.; García-Moreno, I.; Costela, A.; Sastre, R.; Amat-Guerri, F. *Chem. Phys.* **1998**, *236*, 331.
- (16) López Arbeloa, F.; López Arbeloa, T.; López Arbeloa, I. *J. Photochem. Photobiol., A* **1999**, *121*, 177. López Arbeloa, F.; López Arbeloa, T.; López Arbeloa, I. *Recent Res. Dev. Photochem. Photobiol.* **1999**, *3*, 35.
- (17) López Arbeloa, F.; Ruiz Ojeda, P.; López Arbeloa, I. *Chem. Phys. Lett.* **1988**, *148*, 253. López Arbeloa, F.; Ruiz Ojeda, P.; López Arbeloa, I. *J. Chem. Soc., Faraday Trans. 2* **1988**, *84*, 1903.
- (18) Rahn, M. D.; King, T. A.; Gorman, A. A.; Hamblett, I. *Appl. Opt.* **1997**, *36*, 5862.
- (19) Assor, Y.; Burshtein, Z.; Rosenwaks, S. *Appl. Opt.* **1998**, *37*, 4914.
- (20) Costela, A.; García-Moreno, I.; Sastre, R. In *Handbook of Advanced Electronic and Photonic Materials and Devices*; Nalwa, H. S., Ed; Academic Press: San Diego, CA, 2001; Vol. 7, p 161.
- (21) O'Neil, M. P. *Opt. Lett.* **1993**, *18*, 37.
- (22) Rhan, M. D.; King, T. A. *Appl. Opt.* **1995**, *34*, 8260.
- (23) Dubois, A.; Canva, M.; Brun, A.; Chaput, F.; Boilot, J.-P. *Appl. Opt.* **1996**, *35*, 3193.
- (24) Yariv, E.; Schultheiss, S.; Saraidarov, T.; Reisfeld, R. *Opt. Mater. (Amsterdam)* **2001**, *16*, 29.
- (25) Costela, A.; García-Moreno, I.; Gómez, C.; García, O.; Sastre, R. *J. Appl. Opt.* **2001**, *40*, 3159.
- (26) Costela, A.; García-Moreno, I.; Sastre, R.; López Arbeloa, F.; López Arbeloa, T.; López Arbeloa, I. *Appl. Phys. B* **2001**, *73*, 19.
- (27) López Arbeloa, F.; Bañuelos Prieto, J.; López Arbeloa, I.; Costela, A.; García-Moreno, I.; Gómez, C.; Amat-Guerri, F.; Liras, M.; Sastre, R. *Photochem. Photobiol.* **2003**, *78*, 30.
- (28) López Arbeloa, F.; López Arbeloa, F.; López Arbeloa, I.; García-Moreno, I.; Costela, A.; Sastre, R.; Amat-Guerri, F. *Chem. Phys. Lett.* **1999**, *299*, 315.
- (29) López Arbeloa, F.; López Arbeloa, I.; López Arbeloa, T. In *Handbook of Advanced Electronic and Photonic Materials and Devices*; Nalwa, H. S., Ed; Academic Press: San Diego, CA, 2001; Vol. 7, p 209.
- (30) López Arbeloa, I. *J. Photochem.* **1980**, *14*, 97.
- (31) Dewar, M. J. S.; Zoebish, E. G.; Healy, E. F.; Stewart, J. J. P. *J. Am. Chem. Soc.* **1985**, *107*, 3902.
- (32) Stewart, J. J. P. *MOPAC 2000*, version 1.3; Fujitsu: Tokyo, Japan, 2000.
- (33) Baker, J. J. *Comput. Chem.* **1986**, *7*, 385.
- (34) Herradón, B. Personal communication.
- (35) Carretero, L. Personal communication.
- (36) Hofer, J. E.; Grabenstetter, R. J.; Wiig, E. O. *J. Am. Chem. Soc.* **1950**, *72*, 203.
- (37) Bergström, F.; Mikhalyov, I.; Hägglöf, P.; Wortmann, R.; Ny, T.; Johansson, L. B.-A. *J. Am. Chem. Soc.* **2002**, *124*, 196.
- (38) Markus, Y. *Chem. Soc. Rev.* **1993**, 409.
- (39) Reichardt, C. *Chem. Rev.* **1994**, *94*, 2319.
- (40) Catalán, J. *J. Org. Chem.* **1997**, *62*, 8231.
- (41) Lippert, E. In *Organic Molecular Photophysics*; Birks, J. B., Ed; Wiley-Interscience: Bristol, England, 1975, Vol. 2, p 1.
- (42) Dimroth, K.; Reichardt, C. *Liebigs Ann. Chem.* **1969**, 727, 93.
- (43) Kamlet, M. J.; Taft, R. W. *J. Am. Chem. Soc.* **1976**, *98*, 377. Kamlet, M. J.; Taft, R. W. *J. Am. Chem. Soc.* **1976**, *98*, 2886. Kamlet, M. J.; Abboud, J. L. M. Taft, R. W. *J. Am. Chem. Soc.* **1977**, *99*, 6027.
- (44) Catalán, J.; López, V.; Pérez, P. *J. Fluoresc.* **1996**, *6*, 15. Catalán, J.; Palomar, J.; Díaz, C.; de Paz, J. L. *J. Phys. Chem.* **1996**, *101*, 5183. Catalán, J.; Díaz, C. *Liebigs Ann. Recl.* **1997**, 1941.
- (45) Biczók, L.; Bérces, T.; Márta, F. *J. Phys. Chem.* **1993**, *97*, 8895.
- (46) Dunsbach, R.; Schmidt, R. *J. Photochem. Photobiol., A* **1994**, *83*, 7.
- (47) Tittelbach-Helmrich, D.; Steer, R. P. *Chem. Phys.* **1995**, *197*, 99.
- (48) Andersson, P. O.; Bachilo, S. M.; Chen, R.-L.; Gillbro, T. *J. Phys. Chem.* **1995**, *99*, 16199.
- (49) Carvalho, C. E. M.; Brinn, I. M.; Pinto, A. V.; Pinto, M. C. F. R. *J. Photochem. Photobiol., A* **2000**, *136*, 25.
- (50) Drexhage, K. H. In *Dye Lasers Topics*; Schäfer, F. P., Ed; Topics in Applied Physics, Vol. 1; Springer: Berlin, Germany, 1990; p 187.
- (51) Birks, J. B. *Photophysics of Aromatic Molecules*; Wiley-Interscience: London, 1970.
- (52) Allik, T.; Chnadra, S.; Robinson, T. R.; Hutchinson, J. A.; Sathyamoorthi, G.; Boyer, J. H. *Mater. Res. Soc.* **1994**, *329*, 291.
- (53) He, G. S.; Prasad, P. N. *J. Quant. Electron* **1998**, *34*, 473.
- (54) Yariv, E.; Risfeld, R. *Opt. Mater. (Amsterdam)* **1999**, *13*, 49.
- (55) Finlayson, A. J.; Peters, N.; Kolinsky, P. V.; Venner, R. W. *Appl. Phys. Lett.* **1999**, *75*, 457.